Chemical Engineering and Processing 72 (2013) 10–23

Contents lists available at ScienceDirect

Chemical Engineering and Processing: Process Intensification

journal homepage: www.elsevier.com/locate/cep

Manipulation of vapour split in Kaibel distillation arrangements

Maryam Ghadrdan [a], Ivar J. Halvorsen [b], Sigurd Skogestad [a,*]

[a] Department of Chemical Engineering, Norwegian University of Science and Technology, N-7491 Trondheim, Norway
[b] SINTEF ICT, Applied Cybernetics, N-7465 Trondheim, Norway

ARTICLE INFO

Article history:
Received 14 March 2012
Received in revised form 24 March 2013
Accepted 26 June 2013
Available online 4 July 2013

Keywords:
Vapour split
Kaibel column
Manipulated variable

ABSTRACT

In this paper, we want to show how we can gain more from a Kaibel distillation column by considering a degree of freedom which is normally not used. Two methods are used to study the effect of vapour split manipulation, namely a shortcut method and rigorous simulations. Using a case-study, we show that we may not be able to operate close to minimum energy requirement for some feed disturbances as we have the vapour split fixed.

1. Introduction

Thermally coupled distillation arrangements offer direct coupling between the prefractionator and main column which reduce mixing losses and also minimize energy requirement for a specified separation when properly operated. Successful applications of the dividing-wall columns have been reported in industry (e.g. [1]), with BASF, with around 70 columns in operation, as the main user of these columns [2]. In this paper, we study the Kaibel distillation column [3], which may be implemented as a dividing-wall column with two sidestreams. It is a promising energy-saving alternative for separating multi-component mixtures into four potentially pure products.

The vapour split (see Fig. 1) is one of the degrees of freedom in a dividing-wall column. It is usually set at the design phase by determining the location of the wall and the pressure drop in the divided sections, but it is usually not adjustable during operation (e.g. [4]). There is no report from industry of an adjustable vapour split and a degree of freedom in operation is unused. However, to reduce energy usage, several authors including Wolff et al. [5], Halvorsen et al. [6] and Ghadrdan et al. [7] have shown that it is important to set the liquid and vapour splits at their right values.

The Kaibel laboratory setup at NTNU [8] is probably the only implementation of active manipulation of the vapour split. Fig. 2 shows a picture of the lab column with manipulatable vapour and liquid splits. The vapour split valve in this implementation is rudimentary and not very precise, but Dviwedi et al. [9] showed that this can be corrected with a simple temperature feedback action, and the column can be operated and stabilized using the vapour split [9].

The issue of this paper is to further study the potential savings of manipulating the vapour split in the Kaibel arrangements. We study two approaches: First, we have used a very simple and useful tool, called the V_{min} diagram [10], to study the effect of vapour split on the energy requirement. Then, we have confirmed the results by rigorous simulations in UniSim.

2. Degrees of freedom in the Kaibel arrangement

Fig. 1 shows a schematic of a Kaibel dividing-wall distillation column and its thermodynamic equivalent with separate sections. Assuming that the distillate (D) and bottom (B) flows are used for level control, there are six remaining degrees of freedom (u) in a Kaibel distillation column: boilup rate (V), reflux (L), side stream flows (S_1, S_2), liquid split (R_L) and vapour split (R_V).

$$u = [\, R_L \quad R_V \quad L \quad V \quad S_1 \quad S_2 \,]$$

Note that liquid split (R_L) is defined as the ratio of the liquid entering the top of the prefractionator (L_1) to the overall liquid (L) coming from the top of the main column and the vapour split (R_V) is defined as the ratio of the vapour entering the bottom (V_1) of the prefractionator to the overall vapour (V) from the bottom of the main column. Assuming that the objective of the separation is to reach specific product purities, four of the degrees of freedom are used to satisfy the product purity specifications: Top ($x_{D,a}$), side-stream 1($x_{S_1,b}$), side-stream 2 ($x_{S_2,c}$), bottom ($x_{B,d}$). The two

* Corresponding author. Tel.: +47 73594154.
E-mail addresses: ghadrdan@nt.ntnu.no, maryam.ghadrdan@gmail.com (M. Ghadrdan), ivar.j.halvorsen@sintef.no (I.J. Halvorsen), skoge@nt.ntnu.no (S. Skogestad).

0255-2701/$ – see front matter © 2013 Elsevier B.V. All rights reserved.
http://dx.doi.org/10.1016/j.cep.2013.06.014

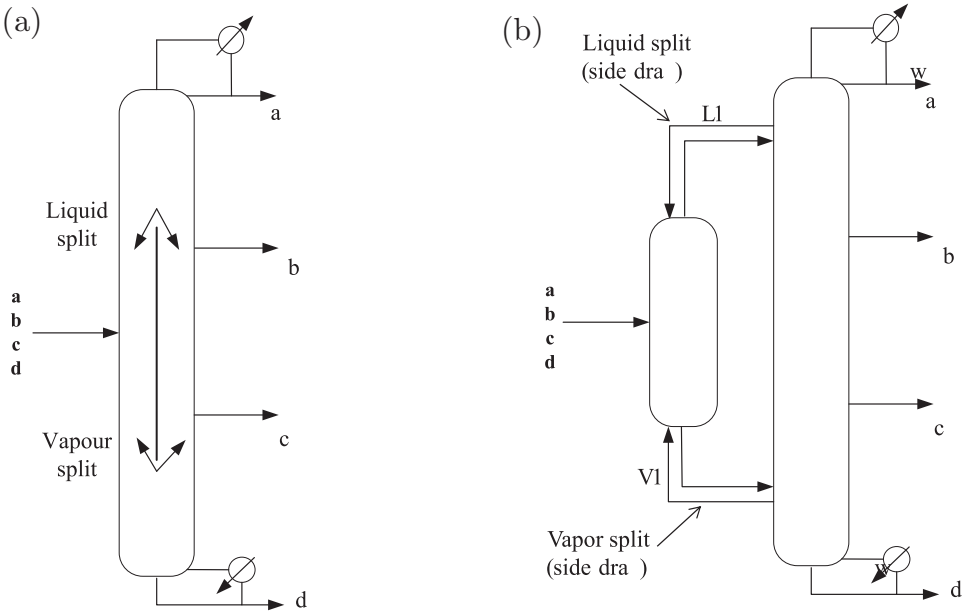

Fig. 1. A schematic of Kaibel dividing-wall distillation column (left) and its thermodynamic equivalent (right).

remaining degrees of freedom can be used for optimization, e.g. for minimizing energy consumption.

3. V_{min} diagrams

In this section, the V_{min} diagram concept is shortly described (for more information please refer to [10,11]). V is the vapour flow in the column, and subscript "*min*" is used because we consider the limiting case with infinite number of stages. The V_{min} diagram gives a lot of insight for design, operation and control of the column and has been successfully used to design thermally coupled columns (e.g. [12]).

3.1. V_{min} diagram basis

The basis for the V_{min} diagram is a conventional two-product distillation column with an infinite number of stages. With a given feed, such a column has two steady-state degrees of freedom. So, the entire operating range can be visualized in two dimensions, even with an arbitrary number of feed components. In the V_{min} diagram, these two dimensions are chosen to be vapour flow per unit feed (V/F) and the product split, expressed by the distillate (D/F). The choice of vapour flow rate on the ordinate provides a direct visualization of the energy consumption and column load. So, for every possible operating point given by the set of recoveries, we want to find the normalized vapour flow rate (V/F), the overall product split (D/F or B/F), and the product distribution.

The V_{min}-diagram in Fig. 3 illustrates how the feed components for a ternary feed (with components a–c) are distributed to the top and bottom products in a simple two-product "infinite stage" distillation column as a function of the product split (D/F). The "mountain-like" boundary ([0,0]-P_{ab}-P_{ac}-P_{bc}-[1,1 − q]) gives V/F when we have pure products. For values above the boundary, we are actually wasting energy. So, an important boundary is the transition from $V > V_{min}$ above boundary to $V = V_{min}$. The peak values give the vapour flow requirement for the corresponding sharp neighbour component splits. The knots (bottom of the valleys) are V_{min} for the so-called "preferred splits" where we specify sharp split between two key components (components a and c), while we allow intermediate components (component b in this example) to be freely distributed. As the vapour flow V is reduced below the boundary for a given D, we no longer have sharp splits. Note that the V_{min} diagram is as exact as the method used to calculate the internal streams. For example, if the Underwood method is used for the shortcut calculation of the internal flows, the underlying assumptions of constant relative volatilities and constant molar flows are required for the V_{min} diagram too. However, the V_{min} diagram can also be generated by simulations for real mixtures (see Section 5). In a general case with N_c components, there are $N_c(N_c-1)/2$ peaks and knots: N_c-1 cases with no intermediates (e.g., a/b, b/c, c/d, . . .) which are the peaks in the V_{min} diagram, N_c-2 cases with one intermediate (e.g., ac, bd, ce, . . .), which are the knots between the peaks. On a first glance of Fig. 3, we can say that the b/c split is the most difficult separation, since it is the highest peak.

3.2. V_{min} diagram for 4-product Petlyuk arrangement

In this paper, we consider the separation of four components. Before deriving the overall minimum vapour flow for the Kaibel column, let us consider the more complex but more energy-efficient extended Petlyuk arrangement for separating four products shown in Fig. 4. The feed specifications and relative volatilities used to sketch the minimum energy diagram in Fig. 4 are:

$$z_F = [0.25 \quad 0.25 \quad 0.25 \quad 0.25]$$
$$q = 1, \text{ (Liquid feed)}$$
$$\alpha = [6.704 \quad 4.438 \quad 2.255 \quad 1]$$

The minimum total vapour flow requirement in a Petlyuk arrangement is given by the highest peak in the V_{min} diagram [10]. For example, the minimum vapour requirement for a 4-component feed (abcd), which is separated into 3 products (a/b/cd) will be

$$V_{T,min,\text{Petlyuk}}(\text{a/b/cd}) = \max(V_{min,2P}(\text{a/b}), V_{min,2P}(\text{b/cd}))$$

where the subscript T refers to the vapour flow in the top of the Petlyuk column, and the subscript $2P$ refers to conventional columns with two products (Fig. 3a). This expression requires that every internal column in the arrangement is operated at its preferred split [13]. All the internal flows can also be obtained from V_{min} diagram

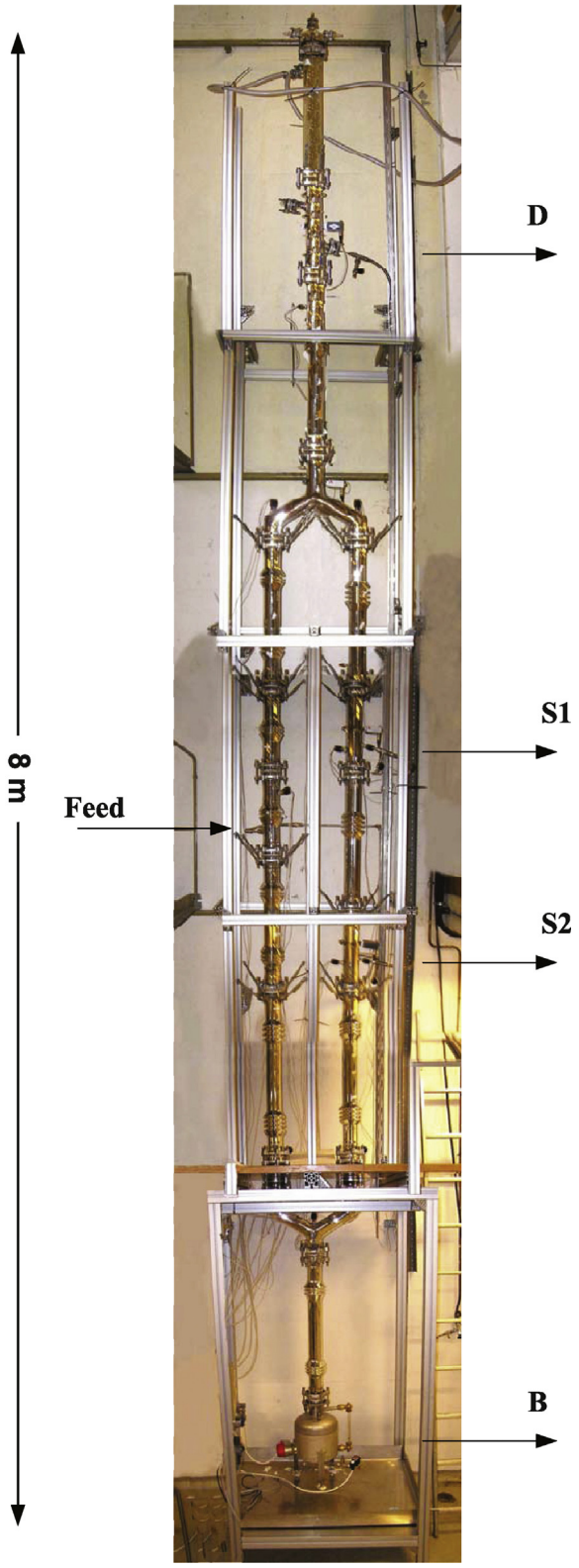

Fig. 2. Laboratory Kaibel distillation column at the Chemical Engineering Department at NTNU, Norway [8].

[14]. Note that the minimum energy which should be provided by the reboiler for the case with constant molar flows is

$$V_{B,\text{Petlyuk}} = V_{T,\text{Petlyuk}} - (1-q)F$$

where q is the liquid feed fraction.

3.3. V_{min} diagram for a Kaibel column

In the Kaibel-arrangement, the prefractionator is not operated at the preferred split, but performs a sharp ab/cd split. The succeeding "main column" performs the a/b split in the top and the c/d split in the bottom. The middle section between the b and c outlet should be operated at full reflux ($V \approx L$) without any net transport of components, since the b/c split is already obtained in the prefractionator. The minimum vapour flow requirement in the main column is given by the highest requirement from the a/b or the c/d split. The minimum vapour flow requirement in the Kaibel column is always outperformed by the full Petlyuk arrangement. This difference can be high or small depending on feed properties [15].

The V_{min} diagram in Fig. 5 (which is identical to the one in Fig. 4) is the V_{min} diagram for the prefractionator of the Kaibel column. As mentioned earlier, the task of the prefractionator is to perform a sharp b/c split. So, the important information to be obtained from the V_{min} diagram in Fig. 5 is the vapour flow V_{1t}, and the net flow D_1 associated with the peak P'_{bc}.

While for the Petlyuk arrangement, all information can be obtained from the standard V_{min} diagram, the Kaibel column requires additional computations for the main column, from which we obtain the corresponding vapour flows V_{2t} and V_{3b} (see Figs. 6 and 7). These are obtained using the approach explained in [15] (see Appendix A).

Fig. 8 shows the final V_{min} diagram for a 4-product Kaibel column made by combining Figs. 5–7. As it is seen from the figure, the most difficult split is taking place in the top main section where we perform the a/b split. So, the total vapour requirement of the column is dictated by the peak P'_{ab} and we have $V_{min} = V_{2t}$. This will lead to excess energy in the other section of the column. Note that from this point on, for the sake of simplicity, we have kept only those parts of the diagram which are specific for the Kaibel distillation column, which correspond to the upper solid line in Fig. 8.

4. Optimal vapour split in Kaibel columns

4.1. Sharp split separation

We first consider the case of a sharp split separation, which means that the lines in V_{min} diagram are for 100% recovery of a component. The following equation is used to calculate the optimal vapour split.

$$R_V = \frac{V_{1t}/F}{V_M/F} \tag{1}$$

where

$$\frac{V_M}{F} = \max(V_{2t}/F, V_{3b}/F).$$

The values of $V_{1t}/F\,(P'_{bc})$, $V_{2t}/F\,(P'_{ab})$ and $V_{3b}/F\,(P'_{cd})$ can be obtained from V_{min} diagram. Fig. 9 shows the V_{min} diagram for three feed composition disturbances, and the corresponding optimal R_V for each case is given in Table 1. It seems that a constant R_V may work fine for a/b feed composition changes, since the vapour requirement in both the prefractionator and main column (peaks P'_{bc} and P'_{ab}) seem to change with about the same ratio. This is shown more clearly in Table 1, where we see that the R_V value is mostly affected by the composition disturbance in the direction of b/c.

In the case when we have a fixed R_V, we need to make sure that the minimum vapour requirement for a b/c sharp separation in the prefractionator is guaranteed. Since the V_{min} diagram is for the optimal R_V, having a fixed R_V means that the vapour requirement for the prefractionator should increase, so that the the ratio of V_{1t} and the corresponding requirement for the main section of the column (V_M) equals the fixed value which is set for R_V. Fig. 10 is an example

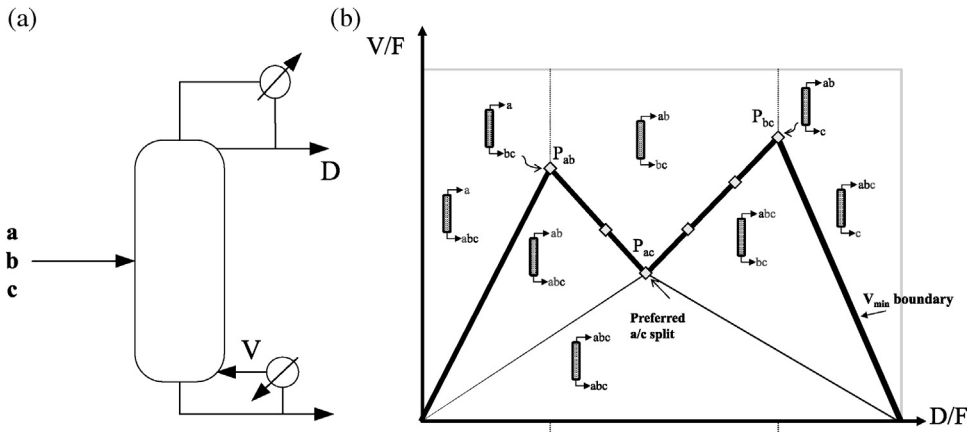

Fig. 3. V_{min} diagram for a ternary feed.

which shows the vapour requirement for the column for a change in feed composition. The optimal R_V for the new feed composition leads to less requirement (In this case: $V_{M,R_{V,opt}} = 2.089$), compared to fixed R_V scenario ($V_{M,R_{V,fixed}} = 2.1535$). This is done by increasing the vapour in the prefractionator (V_{1t}). This in turn will affect the actual Underwood roots and so the vapour requirements in the top and bottom sections of the column (see Appendix A).

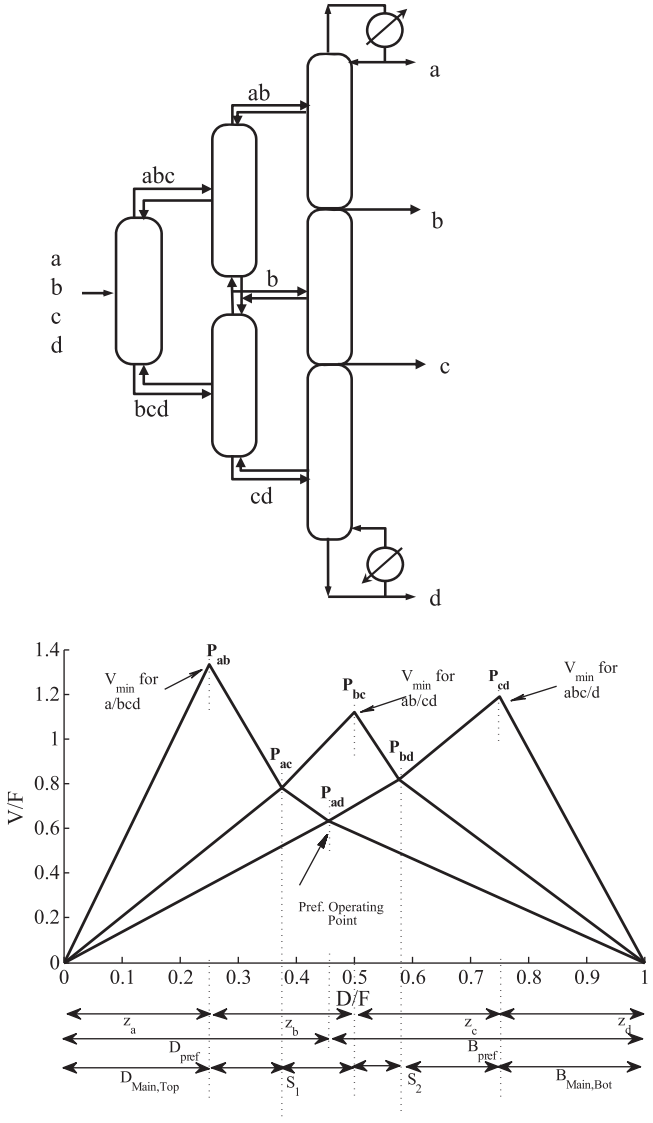

Fig. 4. V_{min} diagram for a 4-product Petlyuk column.

4.2. Non-sharp separation

The analysis becomes more difficult for non-sharp separations. Here, the compositions of component b in the top and c in the bottom of the prefractionator are not zero. We can find a certain slack if we allow non-sharp split in the Kaibel configuration, but this is limited by the product specifications. So, there will be a small region below P_{bc} from which any point could be chosen as the prefractionator's operating point. An optimization can be done to find the best operating point of the prefractionator. Fig. 11 shows an example of non-sharp separation with 95% recoveries for the main products.

The recoveries of the components in all products should be specified in order to sketch the V_{min} diagram. For example, a recovery of 95% for component a in the distillate flow rate does not give any information about the possible existence and the amount of b in this stream. The recoveries of the main products are usually set by the customer needs. By writing the component mass balances around the column and assuming that at optimal operation, the component which is to be drawn at a product stream will only appear in the adjacent product streams and not in the ones away from it (for example, component b which is the main product of S1 stream, will appear as impurity in streams D and S2), we need to estimate two variables to get a feasible solution for mass balance equations. The impurities in products can be guessed from the V_{min} diagram. These issues are dealt in [16]. The highest peak in the V_{min} diagram determines the component that may appear as impurity in the side stream during optimal operation.

5. Rigorous simulation

5.1. V_{min} diagram from rigorous simulation

In this section, we study the minimum energy diagram with a finite (but large) number of stages using rigorous simulations. This is to check the validity of the V_{min} diagrams which are obtained by ideality assumptions.

Table 2 shows the procedure for obtaining the V_{min} diagram using rigorous simulations. Each row in Table 2 corresponds to one line in the V_{min} diagram. For each line, one recovery is fixed. The simulations are done for a conventional column with four components. The recovery can be used as one of the two specifications which are needed to specify the column using the simulator ([17]). The other specification is chosen to be the distillate flow rate.

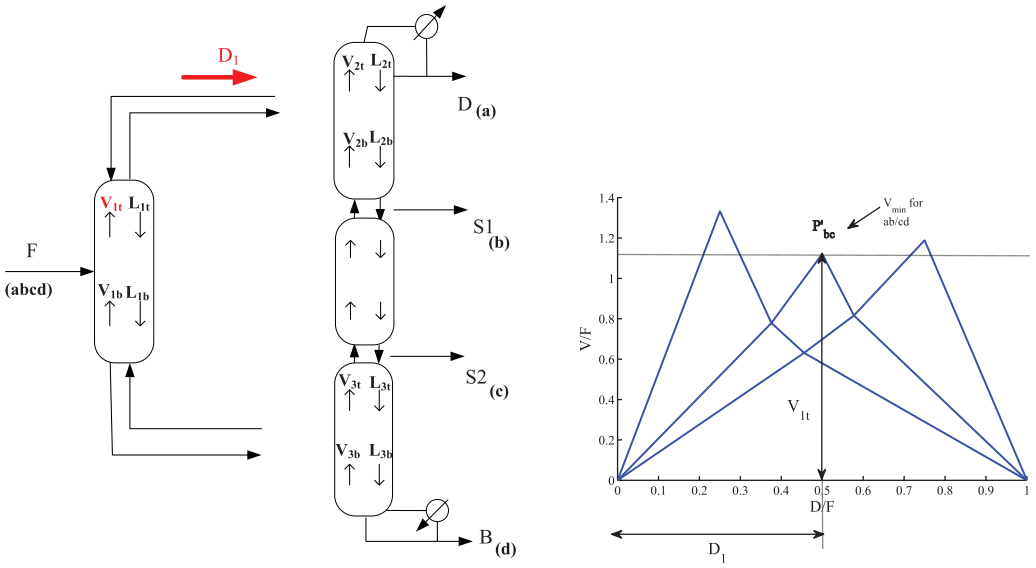

Fig. 5. V_{min} diagram for the prefractionator of Kaibel distillation column (b/c split).

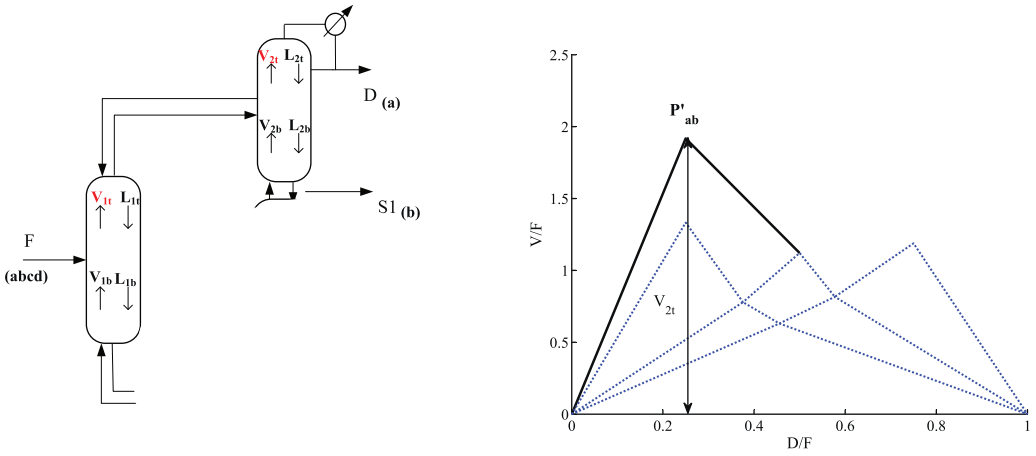

Fig. 6. V_{min} diagram for the top main section of Kaibel distillation column (a/b split).

So, by keeping a recovery constant and increasing the distillate flow rate, the points on each line are obtained. When the recovery specifications for the peaks or valleys are reached, the recovery specifications for the next line should become active to continue the simulation (see Table 2).

In the ideal V_{min} diagram, it is only the peaks and valleys which are calculated. The boundary lines to separate different regions come from connecting these points. This is why the lines go to the origin. For a real column, we should start with a feasible point. This is because it may not be possible to get a certain recovery

Table 1
The optimal values of R_V for different composition disturbances in three main directions.

Disturbance	Feed composition	V_{1t}	V_{2t}	V_{3b}	Optimal R_V
a/b change	[0.20 0.30 0.25 0.25]	1.160	1.995	1.670	0.5815
	[0.25 0.25 0.25 0.25]	1.121	1.918	1.633	0.5846
	[0.30 0.20 0.25 0.25]	1.081	1.838	1.594	0.5882
b/c change	[0.20 0.30 0.25 0.25]	1.059	1.7399	1.671	0.6086
	[0.25 0.25 0.25 0.25]	1.121	1.918	1.633	0.5846
	[0.30 0.20 0.25 0.25]	1.180	2.089	1.591	0.5649
c/d change	[0.20 0.30 0.25 0.25]	1.081	1.886	1.508	0.5733
	[0.25 0.25 0.25 0.25]	1.121	1.918	1.633	0.5846
	[0.30 0.20 0.25 0.25]	1.160	1.949	1.753	0.5952

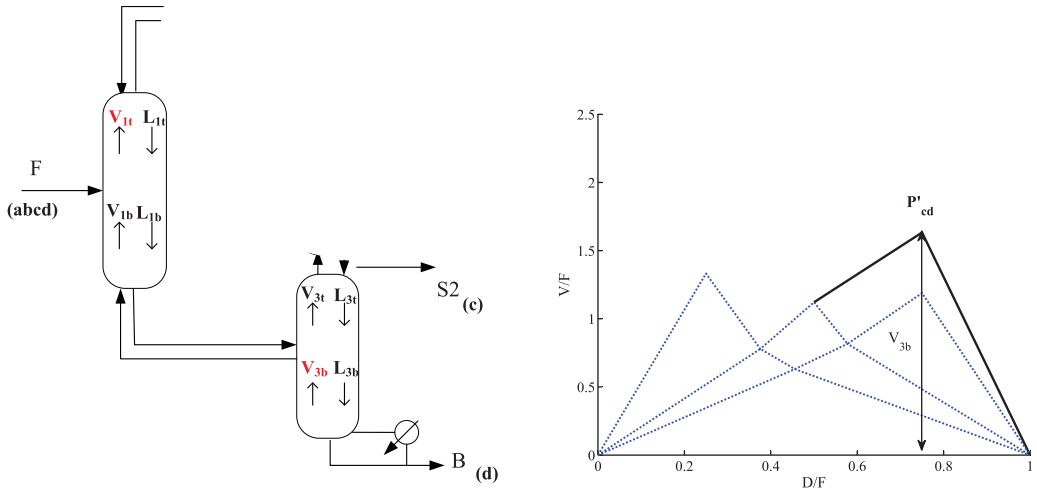

Fig. 7. V_{min} diagram for the bottom main section of Kaibel distillation column (c/d split).

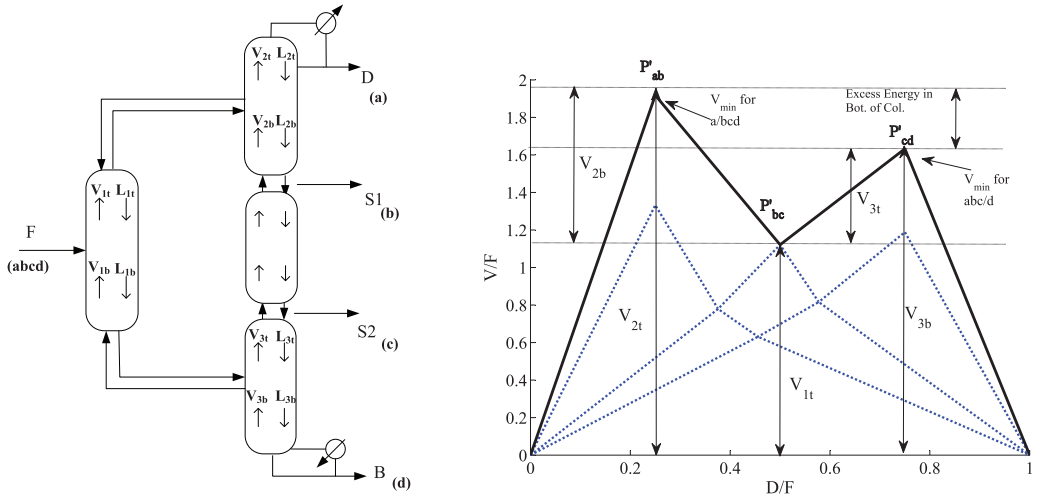

Fig. 8. V_{min} diagram for Kaibel distillation column.

with any amount of distillate flow. We need to start from higher distillate flow rates if the recovery specification is high. The first boundary line is made by specifying the recovery of component b in the bottom ($R_{b,bot}$) at the upper bound (UB). The distillate flow rate is increased until the point where the recovery of component a in the top ($R_{a,top}$) reaches the specified value. The specifications for other boundary lines are given in Table 2.

Table 2
Procedure of constructing the V_{min} diagrams using rigorous simulations.

Line	Specifications
0–a/b,	$R_{b,bot} = UB$, Increase D while $R_{a,top} < UB$
a/b–a/c,	$R_{a,top} = UB$, Increase D while $R_{c,top} < LB$
a/c–b/c,	$R_{c,bot} = UB$, Increase D while $R_{b,top} < UB$
b/c–b/d,	$R_{b,top} = UB$, Increase D while $R_{d,top} < LB$
b/d–c/d,	$R_{d,top} = UB$, Increase D while $R_{c,top} < UB$
c/d–end,	$R_{c,top} = LB$, Increase D while $R_{a,bot} < LB$

R = recovery; UB = upper bound; LB = lower bound.

The infeasible area should be avoided. The area below the line $V = D$ is infeasible since all liquid and vapour streams above and below the feed have to be positive. So, in every step, we should check if the operating point hits the infeasible region or not. The net liquid molar flow in the top section (second stage) is the criterium and it should not become negative. When the $V = D$ line is crossed, we discontinue the current line and the line $V = D$ is followed up to the point where the criterium of the next line is met.

Fig. 12 shows the V_{min} diagrams for a four-component column with fifty stages for different recoveries. It is shown that the difficult split changes depending on the product recoveries. Fig. 13 shows the V_{min} diagrams for 99% recovery for all the main products and with different numbers of stages. As the number of stages become larger, the V_{min} diagram becomes more similar to the ideal V_{min} diagram. As expected, when the number of stages gets relatively

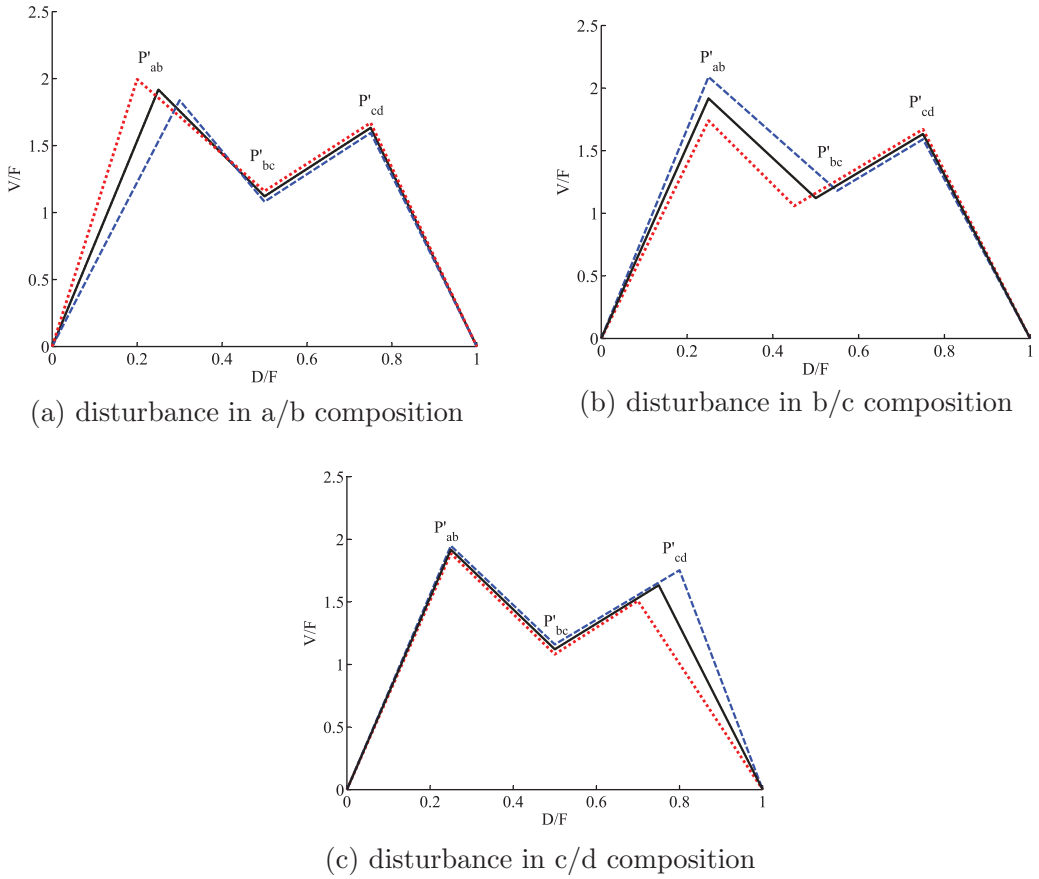

Fig. 9. V_{min} diagram for the Kaibel distillation columns for different feed disturbances. Red: $z_i/z_j = 0.20/0.30$, black: $z_i/z_j = 0.25/0.25$, blue: $z_i/z_j = 0.30/0.20$. (For interpretation of the references to color in this figure legend, the reader is referred to the web version of the article.)

low, the peak V increases sharply. It would go to infinity as we reach N_{min} for the section in question.

5.2. Kaibel case-study

Fig. 14 shows the UniSim simulation flowsheet of a Kaibel column separating four simple alcohols (methanol, ethanol, 1-propanol, 1-butanol). Pumps and valves are needed in the simulations to compensate for the pressure difference between the column sections on the two sides of the wall. In reality, these are not required.

With a given feed, there are six steady-state degrees of freedom. In our case, four degrees of freedom are used to satisfy the four product purities specifications. The remaining two degrees of freedom, here selected as vapour and liquid splits, are used to minimize the energy requirement. Fig. 15 shows contours of constant boilup (V) as a function of the vapour and liquid splits. In a 3-dimensional figure, this looks like a thin bended cone.

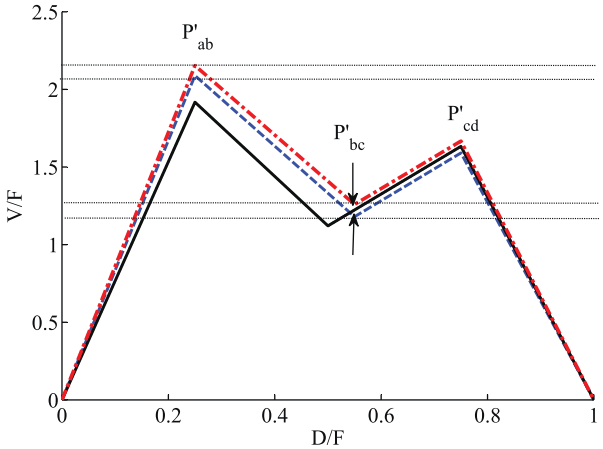

Fig. 10. V_{min} diagram for the nominal feed properties (black, $R_V = 0.5649$) and new feed composition (b/c composition change to 0.30/0.20) with optimal (blue, $R_V = 0.5846$) and fixed R_V(red, $R_V = 0.5649$). (For interpretation of the references to color in this figure legend, the reader is referred to the web version of the article.)

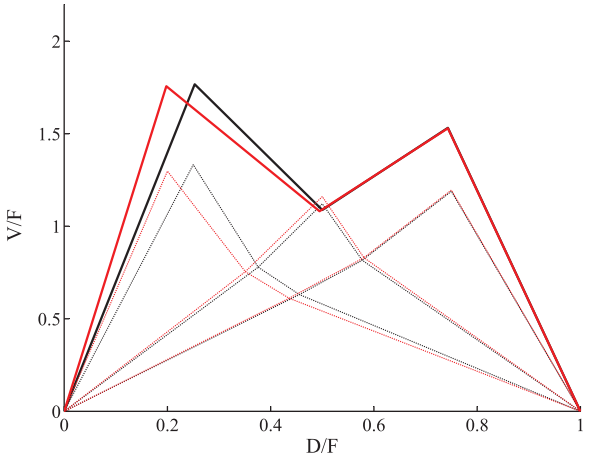

Fig. 11. Nonsharp separation with recovery of 95% for products: equimolar (black) and feed composition of [0.20 0.30 0.25 0.25] (red). (For interpretation of the references to color in this figure legend, the reader is referred to the web version of the article.)

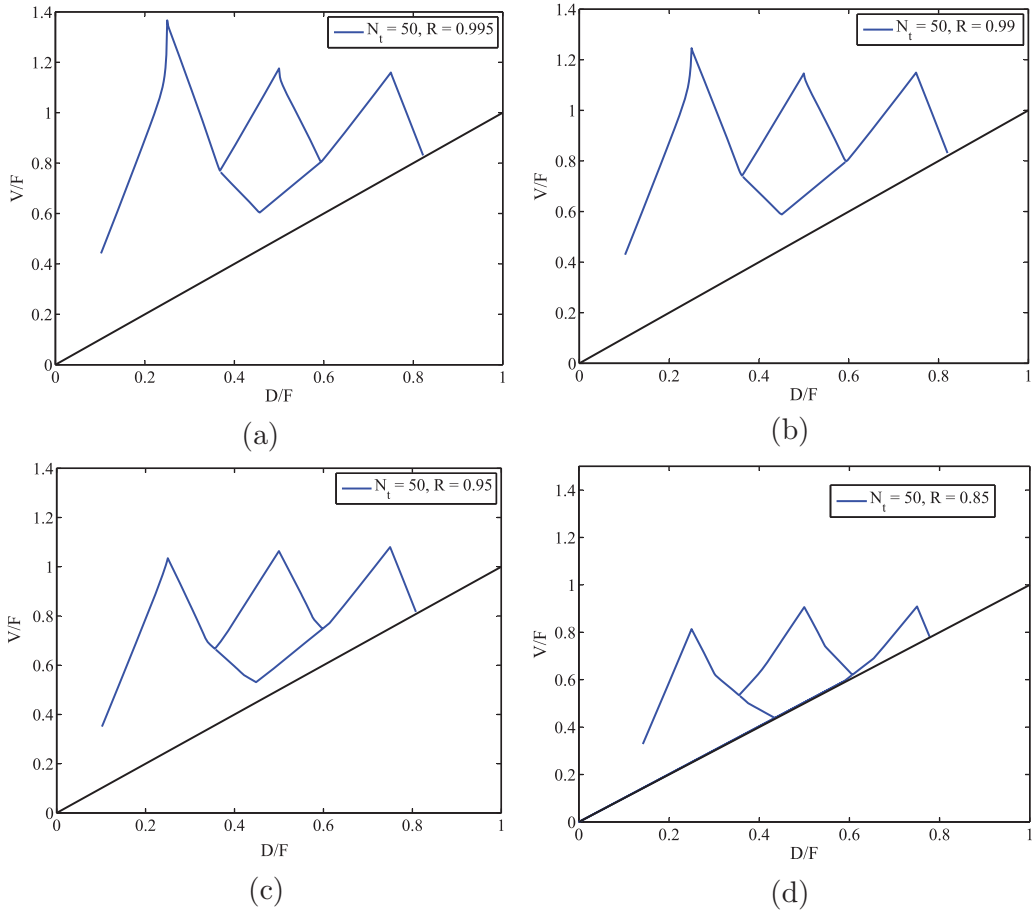

Fig. 12. V_{min} diagrams for different recoveries using rigorous simulations.

Note that the contours for $V > V_{min}$ do not encircle the optimal point for R_L and R_V corresponding to $V = V_{min}$. This is surprising, and implies that there are two solutions for R_L and R_V, where one is undesirable. In Fig. 15 the lower parts of each contour will be undesirable. This may be understood from Fig. 16, which shows a cut of the solution surface at fixed vapour split. From Fig. 16a, we see that the optimal value for R_L is obtained at a minimum value. We also see the multiplicity in the solution, where the upper branch is the undesirable solution. This is further described by Figs. 16 and 17,

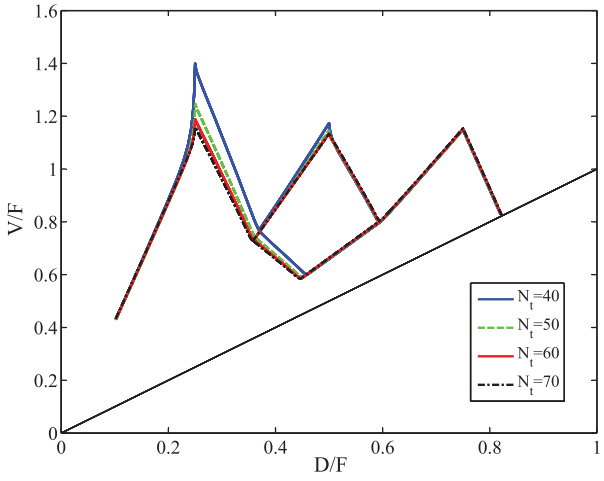

Fig. 13. V_{min} diagrams for 99% recovery with different numbers of trays from rigorous simulations.

which shows that there are two different ways for the components to go to the side-streams and satisfy the product specifications.

In Fig. 18, we study one of the contours and show how the impurities in the top and bottom of the prefractionator and the impurity ratios in the side streams change along the contour. By impurity ratios, we mean x_a/x_c in the $S1$ stream and x_b/x_d in the $S2$ stream. That a/b is the most difficult split can also be seen here, so that impurities of b in the bottom of prefractionator are greater than the impurity of c in the top. This leads to larger ratios of impurities in side stream 1 compared to the impurity ratio in side stream 2. This information could also be obtained from the V_{min} diagram, by finding the column section where we have energy surplus (see Fig. 8). Fig. 18b actually shows many different points that could be picked as the prefractionator's operating point. This was discussed in Section 4.2 and is shown schematically in Fig. 19.

An important point to investigate is to check how much we may lose by keeping R_V constant. To study this, we have plotted in Fig. 20 contours of boilup +2% above the optimal point corresponding to each set of feed compositions for three main directions of composition change. We assume that operating within 2% of minimum energy is still acceptable. The red dots in this figure show the optimum point for each set of feed composition. From Fig. 20, we find that with R_V constant at its nominal value $R_V = 0.6295$, it is possible to operate within 2% of the minimum energy requirement when there are disturbances in the a/b direction and almost possible in the c/d direction. However, as seen from Fig. 20C, this is not the case for a disturbance in the b/c direction. In the figures, we have shown the ranges for R_V that keeps V inside +2% of V_{min} for the disturbances, and for the c/d and b/c disturbances the nominal value of R_V is not in this range. These figures also show that the value of

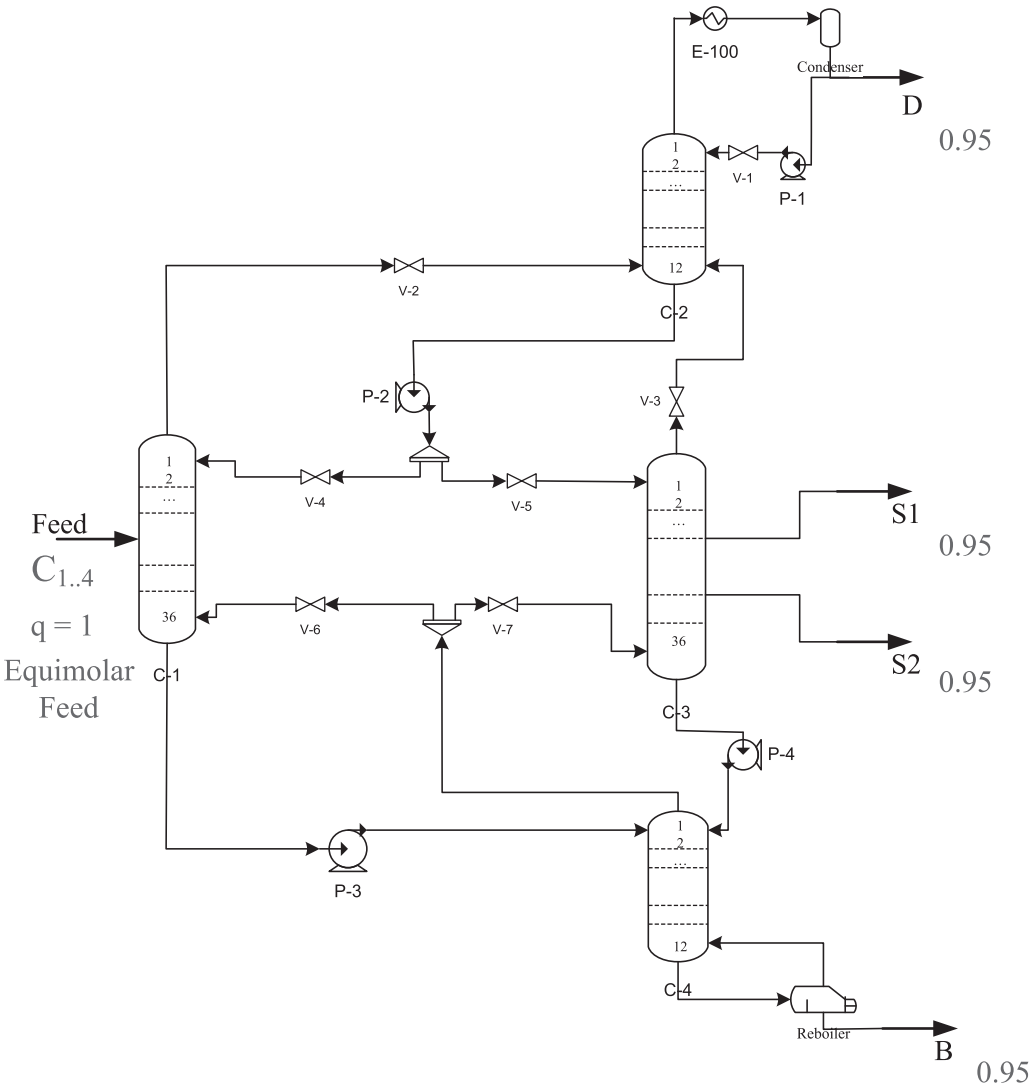

Fig. 14. Simulation flowsheet of Kaibel distillation column.

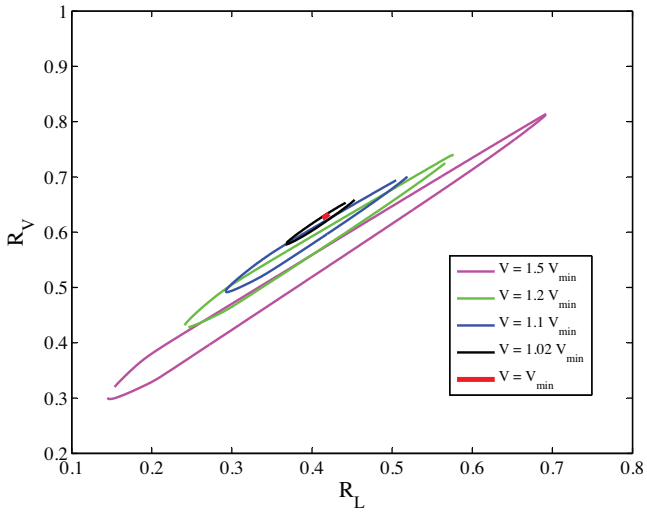

Fig. 15. Contours of constant boilup as a function of vapour and liquid splits at constant product purities.

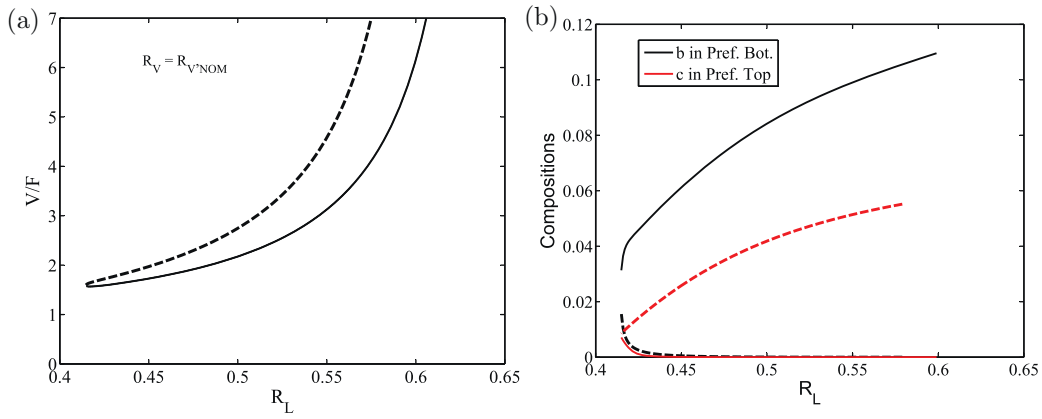

Fig. 16. (a) Boilup rate as a function of liquid split at constant vapour split (R_V = 0.6295) and constant product purities, (b) corresponding impurities in the top and bottom of prefractionator.

a constant vapour split should be chosen carefully so that it covers most of the expected disturbances. As we go further from the minimum requirement, a wider range of disturbances is covered by a fixed R_V, as is shown in Fig. 21, and in this case, the c/d disturbance can be handled by keeping R_V at its nominal value, when we allow for V vary 10% above the minimum.

Fig. 23 shows the comparison between three values of vapour splits: one is the optimal value for the nominal case and the others are some lower and higher value which is chosen by the insight obtained from Figs. 20 and 21. The values in the Figure show the percentage of loss compared to the case that we re-optimize and R_V is a manipulatable variable. It is confirmed that if some lower value

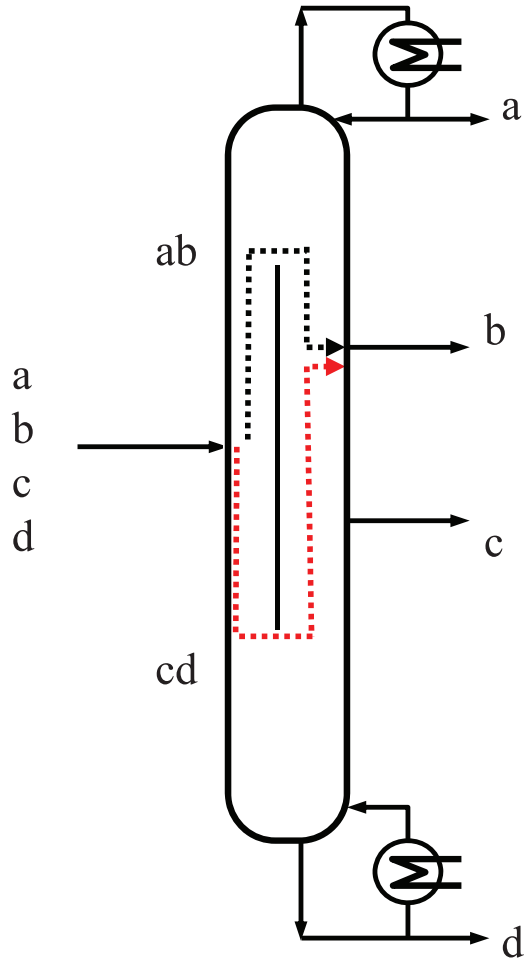

Fig. 17. Paths of component B flow to upper side streams.

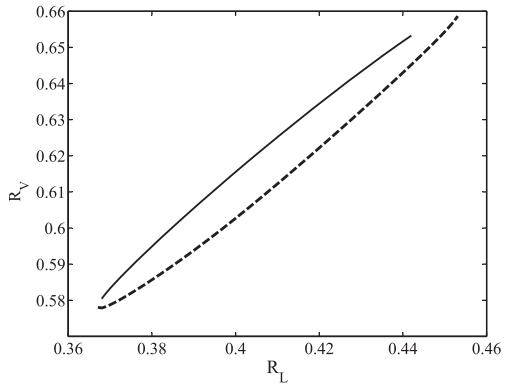

(a) $R_L - R_V$ solution contour for $V = 1\triangleright02V_{min}$

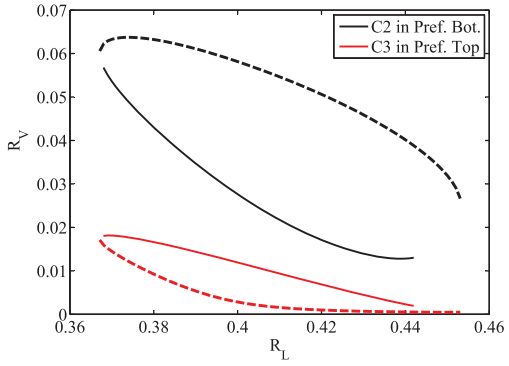

(b) Corresponding impurities in prefractionator's ends

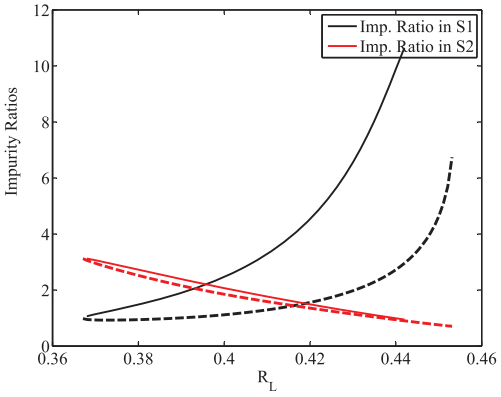

(c) Impurity ratios (light/heavy) in side streams

Fig. 18. Solution properties along a contour of constant vapour boilup ($V = 1.02V_{min}$).

is chosen for the constant R_V, the disturbances in b/c direction are handled better.

The analysis we have done in Figs. 20 and 21 is with the assumption of using additional energy and check if this is sufficient. Another approach would be to check how much additional energy is needed to handle a given a disturbance. Fig. 22 shows plots of boilup (V) versus R_L with fixed R_V. For various feed disturbances, as shown in Fig. 23, the difference in minimum energy consumption is relatively small for the disturbances in a/b (V+ 0.8 %) and c/d directions (V+ 2.8 %). However, the loss is larger if we fix R_V when there are large disturbances in b/c direction (V+ 16.4 %). A large adjustment for R_L is needed to stay at V_{min} (see Fig. 22 C).

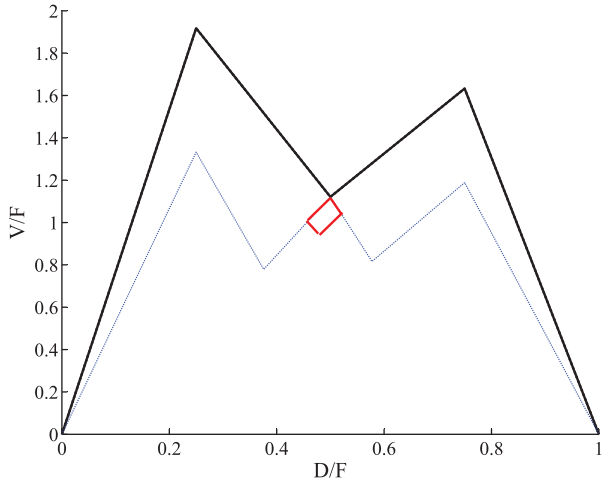

Fig. 19. Degree of freedom for prefractionator operation.

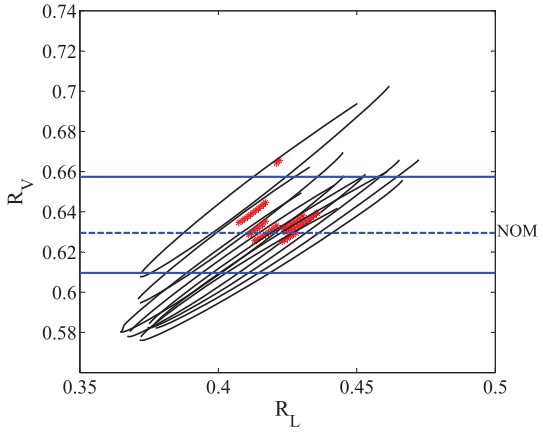

(a) Change in a/b composition (from 0.1/0.4 to 0.4/0.1)

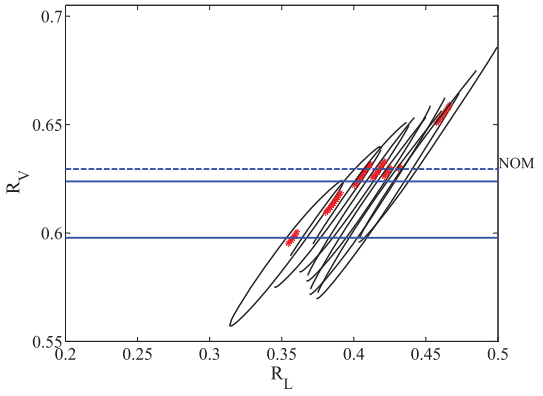

(b) Change in c/d composition (from 0.1/0.4 to 0.4/0.1)

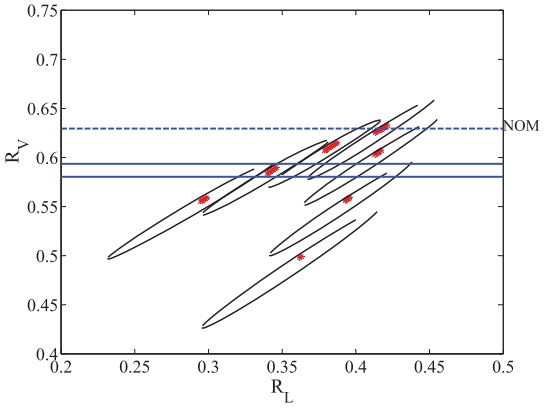

(c) Change in b/c composition (from 0.1/0.4 to 0.4/0.1)

Fig. 20. Contours for boilup +2% above optimal value for different feed composition disturbances. Optimum points for each feed composition in red. (For interpretation of the references to color in this figure legend, the reader is referred to the web version of the article.)

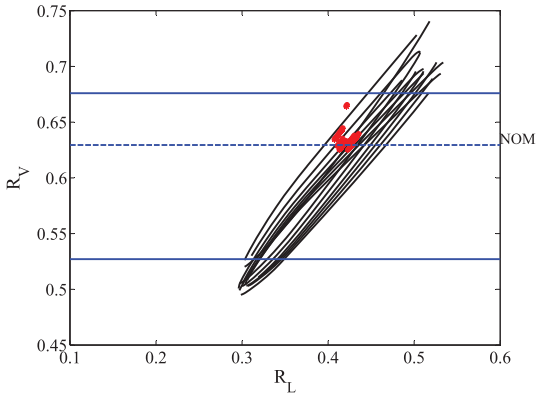

(a) Change in a/b composition (from 0.1/0.4 to 0.4/0.1)

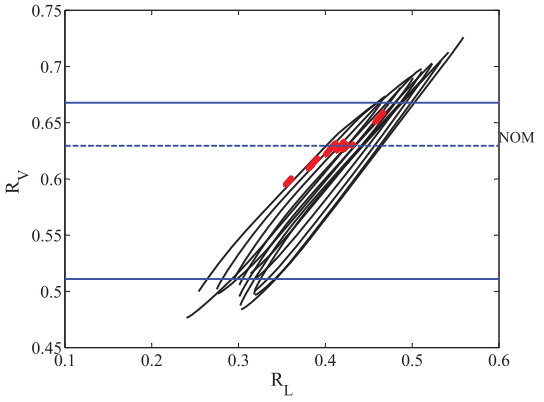

(b) Change in c/d composition (from 0.1/0.4 to 0.4/0.1)

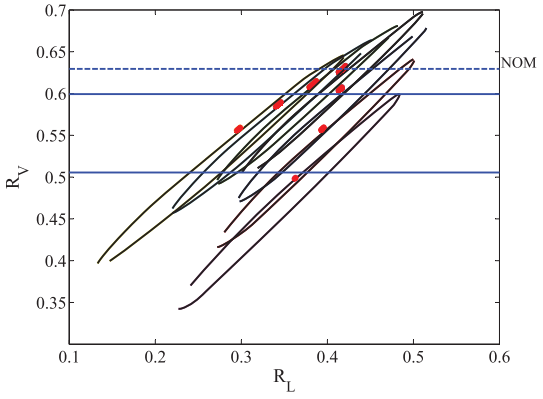

(c) Change in b/c composition (from 0.1/0.4 to 0.4/0.1)

Fig. 21. Contours for boilup +10% above optimal value for different feed composition disturbances. Optimum points for each feed composition in red. (For interpretation of the references to color in this figure legend, the reader is referred to the web version of the article.)

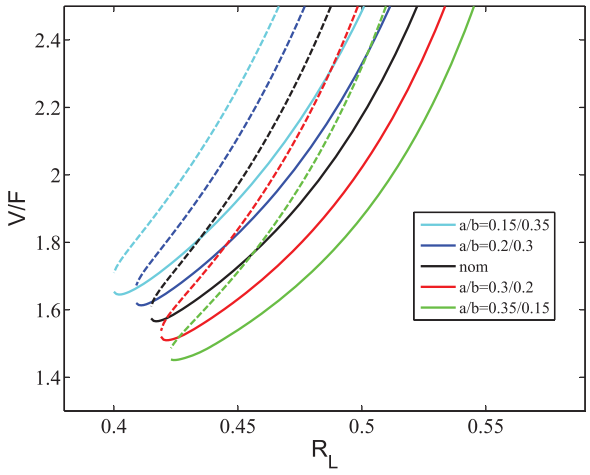

(a) Change in a/b composition

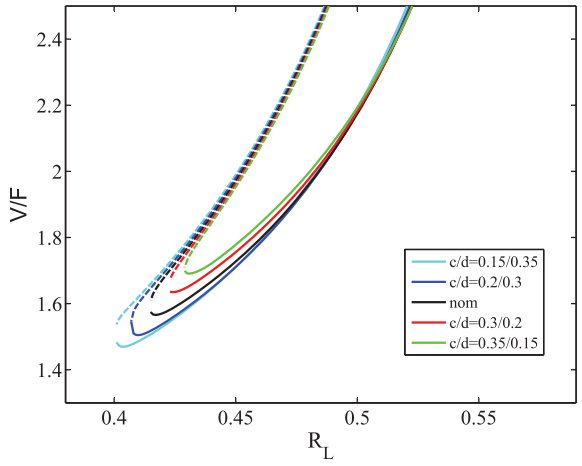

(b) Change in c/d composition

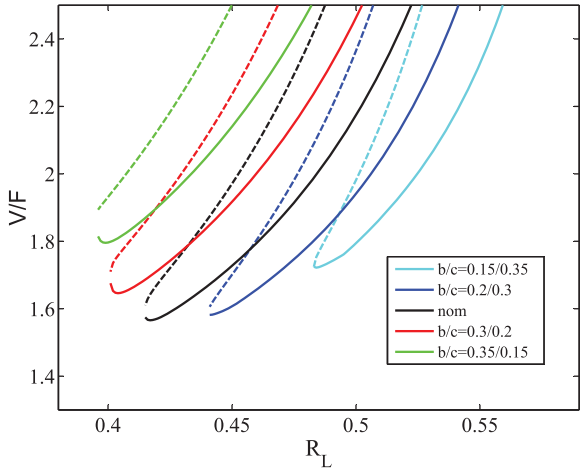

(c) Change in b/c composition

Fig. 22. Solution boundaries for different feed disturbances with fixed R_V (R_V = 0.6295).

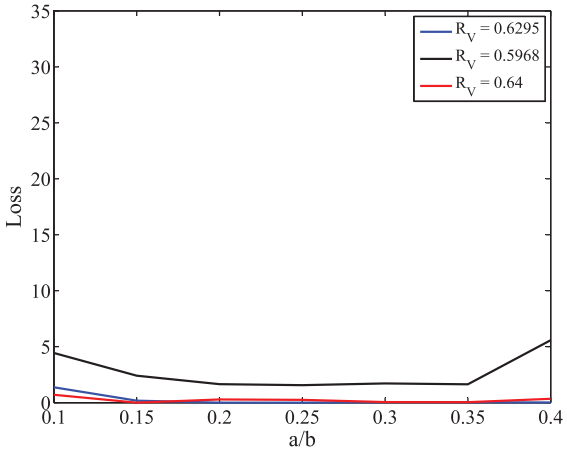

(a) Change in a/b composition

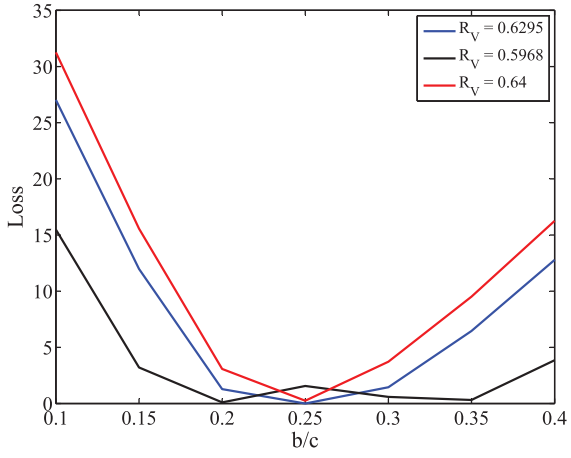

(b) Change in c/d composition

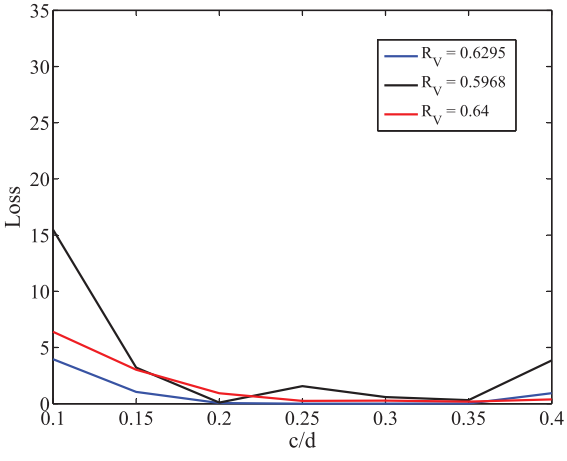

(c) Change in b/c composition

Fig. 23. Loss in energy (V) for different fixed values of R_V: nominal R_V = 0.6295 (blue), lower "optimally" adjusted R_V = 0.5968 (black), higher R_V = 0.64 (red). (For interpretation of the references to color in this figure legend, the reader is referred to the web version of the article.)

However, this may be easy by controlling the composition in the prefractionator.

6. Conclusion

In this paper, we have shown that the realization of the energy saving potential of thermally coupled columns may require on-line adjustment of the vapour split in order to handle expected feed property variations and still maintain minimum energy operation. In particular, this applies to cases where the optimal operating window with a fixed vapour split is narrow, like in a 4-product Kaibel column, and also in some 3-product dividing-wall columns with high purity in the side product. We should pay special attention to disturbances that make the peaks sequence change from one section of the column to the other.

Appendix A. V_{min} diagram for Kaibel column using Underwood equation

In this section, we show how to obtain the minimum vapour flow requirements for Kaibel distillation column from the Underwood equation. This assumes constant relative volatility (α) and constant molar flows. First the Underwood roots are calculated from the below equation.

$$\frac{\alpha_a z_a}{\alpha_a - \theta} + \frac{\alpha_b z_b}{\alpha_b - \theta} + \frac{\alpha_c z_c}{\alpha_c - \theta} + \frac{\alpha_d z_d}{\alpha_d - \theta} = 1 - q \tag{2}$$

The minimum vapour flow rate at the top of the prefractionator is expressed analytically by the Underwood expression [18]:

$$\frac{V_{1t}^{b/c}}{F} = \frac{\alpha_a z_a}{\alpha_a - \theta_b} + \frac{\alpha_b z_b}{\alpha_b - \theta_b} \tag{3}$$

Here θ_b is the middle common Underwood root found from Eq. (2).

In the next step, the actual Underwood root related to the a/b split (ϕ_a) in top of the main section, and the actual Underwood root related to the c/d split (ψ_c) in the bottom of the main section are calculated. They are calculated from the following equations.

$$\frac{V_{1t}^{b/c}}{F} = \frac{\alpha_a z_a}{\alpha_a - \phi} + \frac{\alpha_b z_b}{\alpha_b - \phi} \tag{4}$$

$$\frac{V_{1t}^{b/c}}{F} - (1 - q) = \frac{\alpha_c z_c}{\alpha_c - \psi} + \frac{\alpha_d z_d}{\alpha_d - \psi} \tag{5}$$

The interesting roots are ϕ_a in the top and ψ_c in the bottom. The following equations show the minimum requirements in the top and bottom of the main column [15].

$$\frac{V_{2t}^{a/b}}{F} = \frac{\alpha_a z_a}{\alpha_a - \theta_a^{2t}} = \frac{\alpha_a z_a}{\alpha_a - \phi_a} \tag{6}$$

$$\frac{V_{3b}^{c/d}}{F} = \frac{\alpha_d z_d}{\alpha_d - \theta_a^{3b}} = \frac{\alpha_d z_d}{\alpha_d - \psi_c} \tag{7}$$

References

[1] M.A. Schultz, D.G. Stewart, J.M. Harris, S.P. Rosenblum, M.S. Shakur, D.E. O'Brien, Reduce costs with dividing-wall columns, Chemical Engineering Progress 98 (5) (2008) 64–71.
[2] I. Dejanović, L. Matijašević, Z. Olujić, Dividing wall column - a breakthrough towards sustainable distilling, Chemical Engineering and Processing: Process Intensification 49 (6) (2010) 559–580.
[3] G. Kaibel, Distillation columns with vertical partitions, Chemical Engineering and Technology 10 (1987) 92–98.
[4] M. Abdul Mutalib, R. Smith, Operation and control of dividing wall distillation columns. Part 1. degrees of freedom and dynamic simulation, Transactions on IChemE, Part A (76) (1998) 308–318.
[5] E.A. Wolff, S. Skogestad, Operation of integrated three-product (petlyuk) distillation columns, Industrial and Engineering Chemistry Research 34 (1995) 2094–2103.
[6] I.J. Halvorsen, S. Skogestad, Optimal operation of petlyuk distillation: steady-state behavior, Journal of Process Control 9 (1999) 407–424.
[7] M. Ghadrdan, I.J. Halvorsen, S. Skogestad, Optimal operation of kaibel distillation columns, Chemical Engineering Research and Design 89 (8) (2011) 1382–1391.
[8] J.P. Strandberg, Optimal operation of dividing wall columns, Ph.D. Thesis, Norwegian University of Science and Technology, Department of Chemical Engineering (available from home page of S. Skogestad), 2011.
[9] D. Dwivedi, J. Strandberg, I.J. Halvorsen, S. Skogestad, Steady state and dynamic operation of four-product dividing-wall (kaibel) columns: experimental verification, Industrial and Engineering Chemistry Research 51 (48) (2012) 15696–15709.
[10] I.J. Halvorsen, Minimum energy requirements in complex distillation arrangements, Ph.D. Thesis, Norwegian University of Science and Technology, Department of Chemical Engineering (Available from home page of S. Skogestad) (2001).
[11] I.J. Halvorsen, S. Skogestad, Energy efficient distillation, Journal of Natural Gas Science and Engineering 3 (4) (2011) 571–580.
[12] I.J. Halvorsen, S. Skogestad, I. Dejanović, L. Matijašević, Z. Olujić, Multi-product dividing wall columns: a simple and effective assessment and conceptual design procedure, Chemical Engineering Transactions 25 (2011) 611–616.
[13] J. Stichlmair, Distillation and Rectification, Ullmann's Encyclopedia of Industrial Chemistry, 1988.
[14] I.J. Halvorsen, S. Skogestad, Minimum energy consumption in multicomponent distillation. part 3. more than three products and generalized petlyuk arrangements, Industrial and Engineering Chemistry Research 42 (3) (2003) 616–629.
[15] I.J. Halvorsen, S. Skogestad, Minimum Energy for the Four-product Kaibel-Column, 2006.
[16] M. Ghadrdan, I.J. Halvorsen, S. Skogestad, A shortcut design for kaibel columns based on minimum energy diagrams, Computer Aided Chemical Engineering 3 (4) (2011) 571–580.
[17] Honeywell, Unisim Design r380, 2008.
[18] A.J.V. Underwood, Fractional distillation of multi-component mixtures, Industrial and Engineering Chemistry 41 (12) (1949) 2844–2847.